AAC Accepted Manuscript Posted Online 14 January 2019
Antimicrob. Agents Chemother. doi:10.1128/AAC.01524-18
Copyright © 2019 American Society for Microbiology. All Rights Reserved.

Accepted Manuscript Posted Online
Antimicrobial Agents and Chemotherapy
AAC
Antimicrobial Agents and Chemotherapy

1 # Small molecule inhibitor of FosA expands fosfomycin activity to
2 # multidrug-resistant Gram-negative pathogens

3

4 Running Title: **Small molecule inhibitor of FosA**

5

6 Adam D. Tomich[a¶] , Erik H. Klontz[b,c¶], Daniel Deredge[d], John P. Barnard[a], Christi L.
7 McElheny[a], Megan L. Eshbach[e], Ora A. Weisz[e], Patrick Wintrode[d], Yohei Doi[a,f], Eric J.
8 Sundberg[b,c,g*], Nicolas Sluis-Cremer[a,f*]

9

10 [a]Division of Infectious Diseases, Department of Medicine, University of Pittsburgh School of
11 Medicine, Pittsburgh, Pennsylvania, United States of America
12 [b]Institute of Human Virology, University of Maryland School of Medicine, Baltimore, Maryland,
13 United States of America
14 [c]Department of Medicine, University of Maryland School of Medicine, Baltimore, Maryland,
15 United States of America
16 [d]Department of Pharmaceutical Sciences, University of Maryland School of Pharmacy,
17 Maryland, United States of America
18 [e]Division of Renal-Electrolyte, Department of Medicine, University of Pittsburgh School of
19 Medicine, Pittsburgh, Pennsylvania, United States of America
20 [f]Center for Innovative Antimicrobial Therapy, University of Pittsburgh School of Medicine,
21 Pittsburgh, Pennsylvania, United States of America
22 [g]Department of Microbiology & Immunology, University of Maryland School of Medicine,
23 Baltimore, Maryland, United States of America

Downloaded from http://aac.asm.org/ on January 17, 2019 by guest

Accepted Manuscript Posted Online

AAC
Antimicrobial Agents and Chemotherapy

24 * Corresponding authors e-mails: Nicolas Sluis-Cremer - nps2@pitt.edu; Eric Sundberg -
25 ESundberg@ihv.umaryland.edu
26 ¶These authors contributed equally to this work

27
28
29
30
31
32
33
34
35
36
37
38
39
40
41
42
43
44
45
46

Downloaded from http://aac.asm.org/ on January 17, 2019 by guest

Antimicrobial Agents and Chemotherapy

Accepted Manuscript Posted Online

Antimicrobial Agents and Chemotherapy

AAC

Antimicrobial Agents and Chemotherapy

Downloaded from http://aac.asm.org/ on January 17, 2019 by guest

47 **ABSTRACT**

48

49 The spread of multidrug or extensively drug-resistant Gram-negative bacteria is a serious public
50 health issue. There are too few new antibiotics in development to combat the threat of multidrug-
51 resistant infections, and consequently the rate of increasing antibiotic resistance is outpacing the
52 drug development process. This fundamentally threatens our ability to treat common infectious
53 diseases. Fosfomycin (FOM) has an established track record of safety in humans and is highly
54 active against *Escherichia coli*, including multidrug-resistant strains. However, many other
55 Gram-negative pathogens, including the "priority pathogens" *Klebsiella pneumoniae* and
56 *Pseudomonas aeruginosa*, are inherently resistant to FOM due to the chromosomally-encoded
57 *fosA* gene, which directs expression of a metal-dependent glutathione S-transferase (FosA) that
58 metabolizes FOM. In this study, we describe the discovery and biochemical and structural
59 characterization of 3-bromo-6-[3-(3-bromo-2-oxo-1H-pyrazolo[1,5-a]pyrimidin-6-yl)-4-nitro-
60 1H-pyrazol-5-yl]-1H-pyrazolo[1,5-a]pyrimidin-2-one (ANY1), a small molecule active site
61 inhibitor of FosA. Importantly, ANY1 potentiates FOM activity in representative Gram-negative
62 pathogens. Collectively, our study outlines a new strategy to expand FOM activity to a broader
63 spectrum of Gram-negative pathogens, including multidrug-resistant strains.

64
65
66
67
68
69
70

Accepted Manuscript Posted Online

Antimicrobial Agents and Chemotherapy

AAC

Antimicrobial Agents and Chemotherapy

Downloaded from http://aac.asm.org/ on January 17, 2019 by guest

71 **INTRODUCTION**

72

73 There is a significant clinical and public health burden associated with the increasing prevalence
74 and spread of multidrug-resistant (MDR) or extensively drug-resistant (XDR) Gram-negative
75 bacteria such as carbapenem-resistant and extended-spectrum β-lactamase (ESBL)-producing
76 *Enterobacteriaceae*. These pathogens have been designated a critical priority for antibiotic
77 research and development, as strains are emerging worldwide that cannot be treated with any of
78 the currently available antibiotics. However, a recent report from the World Health Organization
79 highlighted the lack of new potential therapeutic options in the clinical pipeline for multidrug-
80 resistant Gram-negative pathogens [1]. Indeed, nearly all of the agents currently in development
81 are modifications of existing antibiotic classes, and are active only against specific pathogens or
82 a limited set of resistant strains [1]. As such, there is an urgent need to identify more innovative
83 products with no cross- or co-resistance to existing classes of antibiotics.

84

85 Fosfomycin (FOM), a broad-spectrum antibiotic with an extensive track record of safety in
86 humans, exerts its bactericidal activity by covalent attachment to UDP-(*N*-acetyl)glucosamine-3-
87 enolpyruvyl transferase (MurA) [2], the enzyme which catalyzes the first step in cell wall
88 biosynthesis (Fig. 1a). FOM is highly active against *Escherichia coli*, including those producing
89 ESBL [3]. In the United States, a tromethamine FOM formulation is approved as a single-dose,
90 orally administered treatment for acute uncomplicated cystitis. In several European and Asian
91 countries, an intravenous disodium formulation is available, and is used to treat bacteremia,
92 pneumonia, pyelonephritis, osteomyelitis and central nervous system infections, usually in
93 combination with another active agent [4]. In contrast to *E. coli*, many other Gram-negative

Accepted Manuscript Posted Online

Antimicrobial Agents and Chemotherapy

AAC

Antimicrobial Agents and Chemotherapy

94 pathogens including *Klebsiella pneumoniae, Klebsiella oxytoca, Serratia marcescens*,
95 *Enterobacter aerogenes, Enterobacter cloacae, Pseudomonas aeruginosa* and *Morganella*
96 *morganii* are inherently resistant to FOM [5]. This inherent resistance is conferred by a
97 chromosomally-encoded gene, *fosA*, which encodes a dimeric K^+- and Mn^{2+}-dependent
98 glutathione S-transferase (FosA) that catalyzes the nucleophilic addition of glutathione to
99 carbon-1 in the epoxide ring of FOM, rendering the antibiotic inactive (Fig. 1b) [6]. Of note,
100 plasmid-borne *fosA* variants (e.g., *fosA3*) are also emerging as a transferable mechanism by
101 which *E. coli*, which naturally lacks *fosA* as a species, acquires FOM resistance in the clinic [3].
102
103 Inhibition of FosA activity may provide a novel approach to expand the use of FOM to Gram-
104 negative species that produce FosA. A similar approach to expand the use of β-lactam antibiotics
105 has been clinically implemented for many years, following the development and approval of β-
106 lactamase inhibitors such as clavulanic acid, tazobactam, avibactam and vaborbactam. We
107 postulate that FosA is an excellent target for drug discovery because: (i) deletion of
108 chromosomal *fosA* in *S. marcescens* [5], or transposon-mediated disruption of *fosA* in *K.*
109 *pneumoniae* or *P. aeruginosa*, eliminates intrinsic FOM resistance; and (ii) clinically achievable
110 concentrations of foscarnet - a pyrophosphate analog that inhibits DNA polymerases, but also
111 FosA [7] - reduces FOM minimum inhibitory concentrations (MICs) by > 4-fold among
112 representative *K. pneumoniae*, *E. cloacae*, and *P. aeruginosa* clinical strains, and leads to a
113 bacteriostatic or bactericidal effect in time-kill assays [8].
114
115 While foscarnet is approved for the treatment of cytomegalovirus retinitis and refractory
116 mucocutaneous herpes simplex virus infections, its use is associated with significant side effects

Downloaded from http://aac.asm.org/ on January 17, 2019 by guest

Accepted Manuscript Posted Online
AAC
Antimicrobial Agents and Chemotherapy

117 including nephrotoxicity, hypocalcemia, and seizures. Therefore, there is a need to identify and
118 develop selective small molecule inhibitors of bacterial FosA. In this study, we describe the
119 discovery and characterization of a first-in-class, competitive small molecule inhibitor of FosA,
120 which significantly potentiates FOM activity against Gram-negative pathogens that harbor the
121 *fosA* gene.
122
123
124
125
126
127
128
129
130
131
132
133
134
135
136
137
138
139

Downloaded from http://aac.asm.org/ on January 17, 2019 by guest

Antimicrobial Agents and Chemotherapy

Accepted Manuscript Posted Online

Antimicrobial Agents and Chemotherapy

AAC

Antimicrobial Agents and Chemotherapy

Downloaded from http://aac.asm.org/ on January 17, 2019 by guest

140 **RESULTS**

141

142 **Discovery of 3-bromo-6-[3-(3-bromo-2-oxo-1H-pyrazolo[1,5-a]pyrimidin-6-yl)-4-nitro-1H-**
143 **pyrazol-5-yl]-1H-pyrazolo[1,5-a]pyrimidin-2-one (ANY1)**

144 FosA catalyzes the Mn^{2+}- and K^{+}-dependent conjugation of glutathione to carbon-1 of FOM
145 (Fig. 1b) [6]. To quantify FosA activity, we developed an end-point fluorescence-based high
146 throughput screening assay which quantifies glutathione consumption using the thiol reactive
147 dye monochlorobimane (Fig. 1c). The assay is sensitive and robust with a signal-to-noise ratio of
148 8 and a Z'-factor of 0.52. To identify inhibitors of FosA, we screened the ApexScreen library
149 from TimTec (Newark, DE), which contains 5,040 small molecules enriched for chemical
150 diversity and Lipinski Rule parameters (S1 Table). Recombinant purified *K. pneumoniae* FosA
151 ($FosA^{KP}$) was used in the screen. We identified 40 hits with > 50% inhibition (0.8% hit rate).
152 Upon further validation, including dose-response assays, this number decreased to 12. Of these,
153 3-bromo-6-[3-(3-bromo-2-oxo-1H-pyrazolo[1,5-a]pyrimidin-6-yl)-4-nitro-1H-pyrazol-5-yl]-1H-
154 pyrazolo[1,5-a]pyrimidin-2-one (ANY1, Fig. 2a) was the most potent (IC_{50} = 5.1±2.2 μM). The
155 dissociation constant for ANY1 binding to $FosA^{KP}$, measured by isothermal titration calorimetry
156 (ITC; Fig. 2b), was 180 ± 30 nM with a binding stoichiometry of 1:1 ANY1:$FosA^{KP}$ monomer
157 (or 2 molecules of ANY1 for each FosA dimer). In steady-state kinetic assays under near-
158 saturating glutathione concentrations, ANY1 binding increased the Michaelis constant (K_m) for
159 FOM without affecting its maximum rate of reaction (V_{max}; Fig. 2c), whereas under saturating
160 FOM concentrations, ANY1 did not impact the K_m for glutathione binding but decreased V_{max}
161 (Fig. 2d). This pattern of inhibition is consistent with ANY1 acting as a competitive inhibitor of
162 FOM binding, and a noncompetitive inhibitor of glutathione binding.

Accepted Manuscript Posted Online

Antimicrobial Agents and Chemotherapy

AAC

Antimicrobial Agents and Chemotherapy

Downloaded from http://aac.asm.org/ on January 17, 2019 by guest

163 **Crystal structures of FosA^{KP} and FosA3 in complex with ANY1**

164 To understand how ANY1 interacts with FosA, we solved X-ray crystal structures of ANY1
165 bound to FosA^{KP} (3.1 Å) and *E. coli* FosA3 (3.5 Å) (Table 1). Consistent with prior structures
166 [9], both FosA^{KP} and FosA3 display a three-dimensional domain-swapped arrangement of the
167 paired βαβββ-motifs. The amino acid sequence identity between FosA3 and FosA^{KP} is 79% and
168 superimposition of the two enzymes reveals that the overall structure is largely conserved, with a
169 Cα root mean square deviation less than 0.5 Å (Fig. 3a). The basic architecture of the active sites
170 in both FosA proteins, including the essential divalent cation, is also maintained. We found that
171 ANY1 binds at both active sites of FosA^{KP} and FosA3 (Fig. 3b) and, consistent with the kinetic
172 data which showed that it was a competitive inhibitor of FOM (Figs. 2c, 2d), its binding site
173 overlaps with that of FOM (Fig. 3c). Despite the moderate resolution of the datasets, we
174 observed clear electron density for all of the bound ANY1 molecules (Fig. 3d). Furthermore,
175 anomalous bromine signal and high contour electron density maps allowed us to unambiguously
176 assign the locations of both bromine atoms in each of the bound ANY1 molecules (S1 Fig).
177 While ANY1 and FOM share contacts with multiple amino acid residues in FosA (T9, W46,
178 Y65, R122), ANY1 makes unique contacts with additional residues that form the putative
179 glutathione channel (S36, Y39, W46, Y131) (Fig. 3b). All of these residues, shared and
180 unshared, are highly conserved across all FosA enzymes (S2 Table), and introduction of alanine
181 or phenylalanine substitutions at positions 9, 34, 39, 46, 65 and 131 in FosA3 either eliminated
182 or reduced enzyme activity (S2 Fig). Using protein fluorescence quenching, we measured ANY1
183 binding to the mutant FosA3 proteins (Table 1; S2b Fig). The T9A, W34A, S36A, W46A and
184 Y131A substitutions all significantly decreased the affinity of ANY1 for FosA3, further
185 highlighting their role in binding.

Accepted Manuscript Posted Online

Antimicrobial Agents and Chemotherapy

AAC

186 We also observed drug-drug and drug-protein interactions between two adjacent FosA molecules
187 (Fig. 3b, 3d). Despite the fact that ANY1 crystallized with FosA3 and FosA^{KP} under different
188 conditions and in unrelated space groups, these same interactions were observed in both cases.
189 Specifically, there are π-π stacking interactions between the pyrazolopyrimidine rings of two
190 ANY1 molecules bound to adjacent FosA proteins. Additionally, S36 can form hydrogen bonds
191 to either the pyrazole group of the ANY1 molecule in its own active site, or to the
192 pyrazolopyrimidine group of the ANY1 molecule in an adjacent active site (Fig. 3b). In order to
193 determine the importance of these drug-drug and drug-adjacent protein interactions, we solved a
194 1.9 Å-resolution crystal structure of FosA^{KP} bound to 3-bromo-6-(4-nitro-1H-pyrazol-5-yl)-1H-
195 pyrazolo[1,5-a]pyrimidin-2-one (ANY2; S3a Fig), which lacks the pyrazolopyrimidine group
196 that mediates these interactions. As expected, ANY2 binding overlaps with ANY1 binding
197 without forming the same drug-drug or drug-adjacent protein interactions (Fig. 3e, S1c Fig);
198 however its binding affinity, as measured by ITC, was ~22-fold weaker (S3b Fig), thereby
199 suggesting that the drug-drug and drug-adjacent protein interactions observed for ANY1
200 contribute significantly to its binding affinity and activity. Additional structure-activity
201 relationship studies of ANY1 revealed that the pyrazole moiety and the bromines on the
202 pyrazolopyrimidines were required for inhibition of FosA (S4 Fig).
203

204 **Hydrogen-deuterium exchange-mass spectrometry (HDX-MS) of FosA^{KP} in the absence or**
205 **presence of FOM, ANY1 and ANY2**

206 Since X-ray crystallography provides only a static snapshot of ligand binding, we sought to
207 validate our models and explore how substrate and drug binding affects FosA structure and
208 dynamics in solution. To do so, we performed HDX-MS of FosA^{KP} in the presence and absence

Downloaded from http://aac.asm.org/ on January 17, 2019 by guest

Antimicrobial Agents and Chemotherapy

Accepted Manuscript Posted Online

Antimicrobial Agents and Chemotherapy

AAC

Downloaded from http://aac.asm.org/ on January 17, 2019 by guest

209 of FOM, ANY1 and ANY2. HDX-MS relies on the exchange of hydrogen with deuterium on
210 peptide backbone amides, and provides information on backbone solvent accessibility and
211 dynamics, because residues that are more frequently exposed to solvent will undergo faster
212 deuteration. By subtracting the percent deuteration for ligand-bound and unbound $FosA^{KP}$
213 peptides, we determined which regions of the protein displayed statistically significant protection
214 as a result of ligand binding. These regions were then mapped onto the structure(s) of $FosA^{KP}$
215 (Fig. 4). As reported previously, FOM binding decreases deuteration throughout the enzyme;
216 although this is particularly prominent in the K^+-binding loop, glutathione channel, and dimer-
217 interface loop (Fig. 4a) [9]. Overall, FOM and ANY1 display a largely similar HDX protection
218 footprint, consistent with their similar modes of binding (Fig. 4a, 4b). However, in contrast to
219 FOM, ANY1 binding does not impact the K^+-binding loop, consistent with our X-ray crystal
220 structures. The HDX protection of the glutathione binding channel is also different, in that FOM
221 provides greater protection to the β6-α3 loop and α3-helix (residues 115-126), whereas ANY1
222 provides greater protection to the C-terminus of the α3-helix (residues 125-135) and the β2-β3
223 sheets and loop (residues 31-46). This phenomenon could be explained by R122 forming
224 stronger ionic interactions with the phosphate group on FOM, which is more negatively charged
225 than the pyrazolopyrimidine group on ANY1, while S36 and Y131 form interactions with ANY1
226 but not FOM. Finally, FOM and ANY1 differentially impact W46. FOM appears to destabilize
227 W46 as demonstrated by the increase in deuterium uptake; whereas ANY1 stabilizes W46 as
228 indicated by a decrease in deuterium uptake, highlighting the potential importance of the π-
229 halogen bond formed between this residue and ANY1 (Fig. 4C). A comparison of the protection
230 mediated by ANY1 versus ANY2 further supports the potential importance of the additional
231 pyrazolopyrimidine group on ANY1, which may mediate drug-drug and drug-protein

Antimicrobial Agents and Chemotherapy

Accepted Manuscript Posted Online

Antimicrobial Agents and Chemotherapy

AAC

Antimicrobial Agents and Chemotherapy

Downloaded from http://aac.asm.org/ on January 17, 2019 by guest

232 interactions between ANY1 and adjacent active sites (Fig. 4D). While there are no observable
233 interactions between FosA and this additional pyrazolopyrimidine group on the ANY1 molecule
234 in its active site, ANY1 nonetheless offers more protection than ANY2. Furthermore, this
235 protection occurs in the region where the crystal structures predict that ANY1 forms a ~240 $Å^2$
236 protein interface, raising the possibility that the additional pyrazolopyrimidine group on ANY1
237 mediates the formation of this interface in solution.
238

239 **Antibacterial activity of ANY1 alone and in combination with FOM**

240 We evaluated the antimicrobial activity of ANY1, alone and in combination with 32, 64 or 128
241 µg/mL FOM, against the carbapenemase-producing (KPC) clinical strains *K. pneumoniae* I1, *E.*
242 *cloacae* YDC612, *S. marcescens* YDC760-2 and *P. aeruginosa* 75B2 by bacterial growth curve
243 analysis. Each of these clinical strains encodes a chromosomal copy of the *fosA* gene. We also
244 assessed activity against *E. coli* clinical isolate (YD472), a FOM-resistant, ESBL-producing
245 clinical strain that carries a copy of the *fosA3* gene on a plasmid [10]. Growth curves were
246 modeled using a modified 3-parameter Gompertz equation, as described previously [11], which
247 facilitated quantification of the lag time (min), growth rate (OD units/min) and maximum growth
248 (OD units) (S5 Fig). Both the growth rate and maximum growth decreased with increasing
249 concentrations of FOM, which facilitated determination of the FOM concentration required to
250 decrease bacterial growth by 50% (i.e., IC_{50}) (S5c,d Fig).
251

252 We found that bacterial growth of *K. pneumoniae* I1 was significantly attenuated when FOM
253 was combined with ANY1, in a dose dependent manner (Fig. 5a). ANY1 alone had no effect on
254 the growth of *K. pneumoniae* I1 (Fig. 5b), a finding which is consistent with its mechanism of

Accepted Manuscript Posted Online

Antimicrobial Agents and Chemotherapy

AAC

Antimicrobial Agents and Chemotherapy

Downloaded from http://aac.asm.org/ on January 17, 2019 by guest

255 action. However, it potentiated FOM activity in a dose dependent manner, resulting in ~6-fold
256 increase in activity at the highest concentration tested (Fig. 5b). Similar to *K. pneumoniae* I1, the
257 bacterial growth curves of *P. aeruginosa* 75B2, *E. cloacae* YDC612, *S. marcescens* YDC760-2
258 and *E. coli* YD472 were significantly attenuated when 32 μg/mL FOM was combined with
259 ANY1, in a dose dependent manner (Fig. 5c). We next evaluated the effect of a single
260 concentration of ANY1 (112 μg/mL) on FOM activity against *K. pneumoniae* I1, using the
261 growth curve analysis as described above. ANY1 reduced the concentration of FOM required to
262 decrease *K. pneumoniae* I1 maximum growth by 50% ~6-fold ($P < 0.05$): the IC_{50} values for
263 FOM were 144.1 ± 16.5 μg/mL and 23.2 ± 4.3 μg/mL in the absence and presence of ANY1,
264 respectively (Fig. 6a). Time-kill experiments confirmed that ANY1 significantly increased FOM
265 activity (Fig. 6c, d, e). In these time-kill experiments, bacterial regrowth was observed at the 24
266 h time-point when 112 μg/mL ANY1 was combined with 64 or 128 μg/mL FOM (Fig. 6c, d), but
267 not when combined with 256 μg/mL FOM (Fig. 6e). The mechanisms involved in resistance to
268 FOM+ANY1 combinations have yet to be characterized, but we suspect that they most likely
269 involve mutations in GlpT and UhpT transporters that are known to be rapidly selected by FOM
270 *in vitro* [17]. They are, however, unlikely to be clinically significant due to concomitant loss of
271 fitness [18]. In contrast to FOM, ANY1 did not alter the activity of gentamicin, an antimicrobial
272 agent with a mechanism of action distinct from FOM thus used as a control here (Fig. 6b).
273 Importantly, 112 μg/mL of ANY1 also significantly decreased the IC_{50} for FOM for *E. cloacae*
274 YDC612 (23-fold; $P < 0.05$; the IC_{50} values for FOM were 243.3 ± 41.1 μg/mL and 10.4 ± 2.9
275 μg/mL in the absence and presence of ANY1, respectively; Fig. 6f), *S. marcescens* YDC760-2
276 (>100-fold; $P < 0.05$; the IC_{50} values for FOM were > 1000 μg/mL and 16.3 ± 3.4 μg/mL in the
277 absence and presence of ANY1, respectively; Fig. 6g) and FosA3-producing *E. coli* YD472 (1.8-

Accepted Manuscript Posted Online

Antimicrobial Agents and Chemotherapy

AAC

278 fold; P = 0.04; the IC_{50} values for FOM were 102.6 ± 5.3 µg/mL and 56.8 ± 2.4 µg/mL in the
279 absence and presence of ANY1, respectively; Fig. 6h).
280
281 **Toxicity**
282 To evaluate potential cellular toxicity, we assessed the effect of varying concentrations of ANY1
283 (0-224 µg/mL) on the viability of the human-derived kidney epithelial cell line HK2 (Fig. 7a),
284 and of human peripheral blood mononuclear cells (Fig. 7b). HK2 cells were included in this
285 study as the FOM concentrations in urine are exceedingly high (1,000-4,000 µg/mL) following a
286 3 mg oral dose, and therefore we sought to assess toxicity in a kidney cell line. In contrast, the
287 PBMC provide some insight into potential toxicity in the blood. Our results show that ANY1, or
288 combinations of FOM+ANY1, had minimal impact on cell viability, in both cell types, even at
289 the highest concentrations tested.
290
291
292
293
294
295
296
297
298
299
300

Downloaded from http://aac.asm.org/ on January 17, 2019 by guest

Antimicrobial Agents and Chemotherapy

Accepted Manuscript Posted Online
Antimicrobial Agents and Chemotherapy
AAC
Antimicrobial Agents and Chemotherapy
Downloaded from http://aac.asm.org/ on January 17, 2019 by guest

301 **DISCUSSION**

302

303 The spread of MDR or XDR Gram-negative bacteria is a serious public health issue [12]. FOM
304 has a strong track record of safety in humans with no cross-resistance to other antibiotics, and is
305 one of the drugs that have been proposed as part of combination regimens for the treatment of *K.*
306 *pneumoniae* carbapenemase (KPC)-producing *K. pneumoniae* infections [13]. However, in
307 comparison to *E. coli*, many Gram-negative bacteria including *K. pneumoniae* exhibit intrinsic
308 resistant to FOM due to inherent expression of FosA [5], an enzyme that catalyzes the
309 nucleophilic addition of glutathione to carbon-1 of the epoxide ring of FOM, rendering the
310 antibiotic inactive. In this regard, inhibition of FosA could help to expand the activity of FOM
311 against Gram-negative bacteria that inherently express this enzyme. In support of this hypothesis,
312 deletion of chromosomal *fosA* in *S. marcescens* [5], or transposon-mediated disruption of *fosA* in
313 *K. pneumoniae* and *P. aeruginosa*, eliminates intrinsic FOM resistance (S3 Table).

314

315 Using an in *vitro* biochemical HTS assay we identified ANY1, which binds to the active site of
316 the enzyme and inhibits FOM metabolism. A key feature of ANY1 is that it exhibits antibacterial
317 activity against representative Gram-negative pathogens, including *K. pneumoniae,* when
318 combined with FOM (Fig 5), but not gentamicin (Fig 5f), highlighting its specificity as a FOM
319 potentiator. In contrast, most *in vitro* HTS campaigns have failed to identify small molecule
320 inhibitors with antibacterial activity largely due to their poor penetration into Gram-negative
321 pathogens [14]. In this regard, Richter *et al.* recently described a set of physicochemical
322 properties that enable small molecules to accumulate in Gram-negative bacteria [15].
323 Interestingly, ANY1 harbors many of these described properties including the presence of an

Accepted Manuscript Posted Online

Antimicrobial Agents and Chemotherapy

AAC

Antimicrobial Agents and Chemotherapy

Downloaded from http://aac.asm.org/ on January 17, 2019 by guest

324 amine, an amphiphilic and rigid structure, and low globularity. In Fig 5 and 6, we show that
325 ANY1 potency varies across different pathogens with potent activity against *K. pneumoniae* I1,
326 *E cloacae* YD612 and *S. marcescens* YD6760-2 (Fig 5g, 5h, 5i) and weaker activity against *E.*
327 *coli* YD472 (Fig 5j). Given that the ANY1 binding and inhibition constants are similar for
328 purified $FosA^{KP}$ and FosA3, these differences in antibacterial potency are likely driven by
329 differences in the intracellular penetration of ANY1 into the different Gram-negative pathogens.
330 Importantly, the crystal structures of FosA in complex with ANY1 described in this study
331 provide a platform for structure-guided drug design to potentially improve inhibitor binding
332 affinity. For example, ANY1 could be modified such that it interacts with residues that form the
333 K^+-binding loop (K93, S97, Y103) which are critical for FOM binding and enzyme function
334 (Fig. 3c) [16].
335
336 ANY1 binds in the active site of FosA and interacts with amino acid residues which are highly
337 conserved throughout the FosA superfamily (S2 Table), thus suggesting a high genetic barrier to
338 resistance for a FOM/ANY1 drug combination. However, FOM resistance can also be conferred
339 by mechanisms other than *fosA*, including mutation of the conserved cysteine residue in the
340 active site of MurA, or the development of mutations in the bacterial glycerol-3-phosphate
341 (GlpT) or glucose-6-phosphate (UhpT) transporters resulting in reduced FOM permeability [3].
342 Mutation of the active site cysteine in MurA has only been documented *in vitro* for clinically
343 relevant Gram-negative bacteria [17,18], and has not been observed clinically. Mutations in
344 GlpT and UhpT are known to be a mechanism of *de novo* resistance to FOM *in vitro* [17] but
345 they are unlikely to be clinically significant due to concomitant loss of fitness [18].
346

Accepted Manuscript Posted Online

Antimicrobial Agents and Chemotherapy

AAC

Antimicrobial Agents and Chemotherapy

Downloaded from http://aac.asm.org/ on January 17, 2019 by guest

347 In conclusion, in this study we describe the discovery and characterization of a novel,
348 competitive small molecule inhibitor of FosA, which significantly potentiates FOM activity in
349 representative Gram-negative pathogens. However, additional studies focused on the
350 pharmacology, pharmacokinetics and resistance development of ANY1 are needed to
351 comprehensively assess the therapeutic potential of this compound. Nonetheless, this study
352 shows that combination of a FosA inhibitor, such as ANY1, and FOM provides a new strategy to
353 expand FOM activity to a broader spectrum of Gram-negative pathogens, including MDR and
354 XDR strains.
355
356
357
358
359
360
361
362
363
364
365
366
367
368
369

Accepted Manuscript Posted Online

Antimicrobial Agents and Chemotherapy

AAC

Antimicrobial Agents and Chemotherapy

Downloaded from http://aac.asm.org/ on January 17, 2019 by guest

370 **MATERIALS AND METHODS**

371

372 **Protein expression and purification**

373 The *fosA*^{KP} and *fosA3* genes (including mutants) were synthesized with the inclusion of a C-

374 terminal His_6 tag by Genscript (Piscataway, NJ, USA), and cloned into pET-22(b+) for protein

375 expression and purification, as described previously [9].

376

377 **FosA assays**

378 FOM-dependent glutathione conjugation was detected spectrophotometrically using

379 monochlorobimane (Sigma-Aldrich) to detect unreacted free glutathione (Fig 1c). Assays were

380 carried out in a volume of 50 µL at 25°C in 0.1 M sodium phosphate buffer pH 8.0 containing 50

381 mM KCl, 25 µM $MnCl_2$, 30 mM glutathione and varying concentrations of fosfomycin (0-50

382 mM). 100 nM FosA was used to initiate the reaction, which was quenched after 20 min. A no-

383 enzyme control was also performed. Reactions were quenched by the addition of 150 µL

384 methanol for 30 min, and then diluted 100-fold in 0.1 M sodium phosphate buffer pH 8.0

385 containing 1 mM EDTA. Following the addition of 500 µM monochlorobimane (1.7-fold molar

386 excess of monochlorobimane to glutathione), and a 2 h incubation period, the concentration of

387 glutathione was established by fluorescence spectroscopy using a SpectraMax M2 Plate reader

388 (Molecular Devices). Excitation and emission wavelengths of 390 nm and 478 nm, were used

389 respectively. A standard curve was prepared using 0-750 µM glutathione. Data were fit to

390 Michaelis-Menten equations using SigmaPlot (Systat Software Inc, San Jose, CA).

391

392 **Isothermal Titration Calorimetry**

Accepted Manuscript Posted Online

393 Experiments were performed using an iTC200 instrument (GE Healthcare), using a syringe
394 loaded with ligand (250-500 µM) and a cell loaded with $FosA^{KP}$ (15-30 µM) in 75mM NaCl,
395 10mM Tris pH 7.8. Titrations were performed at 25°C with 16 injections of 2.42-µL aliquots,
396 with 230 s intervals between injections. All runs were performed in triplicate and heats of
397 dilutions were measured and subtracted from each dataset. All data were analyzed using Origin
398 7.0 software. Uncertainty in ANY1/ANY2 concentrations led to binding ratios that varied from
399 0.8-0.9 [(ligand)/($FosA^{KP}$ monomer)], which were subsequently fixed to equal 1 based on X-ray
400 crystal structures.

401 **Protein crystallization**

402 FosA3 was concentrated to 12 mg/mL and combined with 2.5 mM ANY1, 6 mM $MnCl_2$, and
403 100 mM KCl. This was centrifuged (19,150 x g for 10 min) and 250 nl of the supernatant was
404 combined with 250 nl of mother liquor (0.2 M magnesium formate, 20% [w/v] polyethylene
405 glycol 3350) in sitting drops. $FosA^{KP}$ was concentrated to 12 mg/mL, combined with 2.5 mM
406 ANY1, 6 mM $MnCl_2$, and 100mM KCl, and centrifuged (19,150 x g for 10 min). One microliter
407 of supernatant was combined in hanging drops with 1 µl of mother liquor (0.02 M $CaCl_2$, 0.1 M
408 sodium acetate pH 4.6, 30% [v/v] 2-methyl-2,4-pentanediol). Finally, 1.25 mM ANY2 and 500
409 µM $MnCl_2$ was added to an 11.5 mg/mL stock solution of $FosA^{KP}$, centrifuged (19,150 x g for 10
410 min) and 1 µl of the supernatant was combined in hanging drops with 1 µl of mother liquor (0.2
411 M ammonium sulfate, 0.1 M bis-tris pH 5.5, 20% [w/v] polyethylene glycol 3350). Resulting
412 crystals were improved by streak seeding. Crystals were harvested and flash cooled with liquid
413 nitrogen in mother liquor (ANY1-$FosA^{KP}$) or mother liquor supplemented with 20% (v/v)
414 glycerol as cryoprotectant (ANY2-$FosA^{KP}$ and ANY1-FosA3).
415

Downloaded from http://aac.asm.org/ on January 17, 2019 by guest

Antimicrobial Agents and Chemotherapy
AAC
Antimicrobial Agents and Chemotherapy

Accepted Manuscript Posted Online

Downloaded from http://aac.asm.org/ on January 17, 2019 by guest

416 **X-ray diffraction, data processing, structure determination, and refinement**

417 X-ray diffraction data for FosA3 in complex with ANY1 were collected using a Dectris EIGER
418 X 16M detector on APS beamline 23-ID-B. Data sets were collected at native wavelength
419 (1.0332 Å) as well as the K-edge of bromine (0.91 Å) to facilitate construction of anamolous
420 maps. Data for $FosA^{KP}$ in complex with ANY1 were collected using a Dectris PILATUS3 S 6M
421 detector on SSRL beamline 12-2. Data for $FosA^{KP}$ in complex with ANY2 were collected using a
422 Dectris PILATUS3 S 6M detector on SSRL beamline 9-2. All datasets were processed using
423 XDS, scaled in AIMLESS, and solved by molecular replacement using PHENIX-MR with apo
424 FosA3 (PDB accession code 5VB0) [9] as the search model for the ANY1-FosA3 structure and
425 fosfomycin-bound $FosA^{KP}$ (PDB accession code 5V3D) [9] as the search model for the ANY1-
426 $FosA^{KP}$ and ANY2-$FosA^{KP}$ structures. The ANY1-$FosA^{KP}$ dataset was significantly anisotropic
427 along one of the axes between 3.2-5 Å, resulting in higher than normal R_{merge} values. R_{merge}
428 values could be restored to typical ranges (~0.18) by cutting the resolution to 5 Å, however loss
429 in map clarity led us to include the higher resolution data. Models were further built and refined
430 using Coot and PHENIX, respectively. The locations of the heavy atoms (zinc and bromine)
431 were determined from the ANY1-FosA3 dataset by removing all ligands from the structure, and
432 using PHENIX Phaser-EP MR-SAD to find the location of zinc and bromine atoms. Two zinc
433 and four bromine atoms were found, with a figure or merit of 0.747 and log-liklihood gain of
434 565, with locations matching as expected.

435

436 **Accession Numbers**

437 The atomic coordinates have been deposited in the Protein Data Bank, www.pdb.org (PDB ID
438 codes 6C3U, 5WEW, and 5WEP).

AAC

Antimicrobial Agents and Chemotherapy

Antimicrobial Agents and Chemotherapy

Accepted Manuscript Posted Online

Antimicrobial Agents and Chemotherapy

AAC

Antimicrobial Agents and Chemotherapy

Downloaded from http://aac.asm.org/ on January 17, 2019 by guest

439 **HDX-MS**

440 HDX-MS was performed as previously described [9], with the following modifications.
441 For ANY1, 3 µl of 50 µM $FosA^{KP}$ + 100 µM ANY1 in 20 mM Tris (pH 7.8), 150 mM KCl, and
442 50 µM $MnCl_2$ was deuterated with 27 µl of 20 mM Tris, 99.99% D_2O (pD 7.8), 150 mM KCl, 50
443 µM $MnCl_2$ prior to quenching. For ANY2, 3 µl of 50 µM $FosA^{KP}$ + 100 µM ANY1 in 20 mM
444 Tris (pH 7.8), 150 mM KCl, and 50 µM $MnCl_2$ was deuterated 27 µl of 20 mM Tris, 99.99%
445 D_2O (pD 7.8), 150 mM KCl, 50 µM $MnCl_2$ and 125µM ANY2. Statistical confidence was
446 determined as previously described [8]. Briefly, confidence intervals for the Δ%D plots were
447 determined using the method outlined by Houde *et al*. [22].

448

449 **Fluorescence Binding Assays**

450 ANY1-dependent quenching of the wild type and mutant FosA protein fluorescence was detected
451 using an FP-8500 spectrofluorometer (JASCO, Easton, MD). Assays were carried out in a total
452 volume of 600 µL at 25°C in 0.1 M sodium phosphate buffer (pH 8.0) containing 100 nM FosA
453 and vary concentrations of ANY1 (0-5 µM). Excitation and emission wavelengths of 280 nm and
454 311 nm, were used, respectively. To correct for inner-filter and dilution effects, quenching data
455 were adjusted based on control assays that were performed using a solution of L(-)-tryptophan
456 (ACROS Organics) that was diluted to approximately match initial fluorescence of the protein
457 solutions. Adjusted fluorescence quenching data were fit to a simple hyperbolic binding equation
458 using SigmaPlot (Systat Software Inc, San Jose, CA)

459

460 **Bacterial growth curve analysis**

Accepted Manuscript Posted Online

Antimicrobial Agents and Chemotherapy

AAC

Antimicrobial Agents and Chemotherapy

Downloaded from http://aac.asm.org/ on January 17, 2019 by guest

461 Overnight culture of the clinical isolates *K. pneumoniae* I1, *P. aeruginosa* 75B2, *E. cloacae*
462 YDC612, *S. marcescens* YDC760-2 or *E. coli* YD472 were grown in Mueller-Hinton Broth at
463 37°C, 150 rpm. *E. coli* YD472 is a previously reported strain that produces plasmid-encoded
464 FosA3 along with CTX-M-65 ESBL. *K. pneumoniae* I1 and *E. cloacae* YDC612 are
465 carbapenem-resistant strains that produce KPC-type carbapenemase and were isolated from
466 blood and a hematoma, respectively. *P. aeruginosa* 75B2 is a carbapenem-resistant strain from a
467 urine culture. All strains were from clinical specimens obtained from patients at the University of
468 Pittsburgh Medical Center. The following day, the culture was diluted such that its OD_{600} was
469 0.2. The diluted culture was allowed to grow at 37°C for 1 h. Following this, the culture was
470 further diluted into 96-well, round-bottom plates such that the OD_{600} was 0.1. Varying
471 concentrations of ANY1 (0-224 μg/mL) or FOM (0-1024 μg/mL) were added in addition to 25
472 μg/mL glucose-6-phosphate. The plate was incubated at 37°C for up to 300 min. The OD_{600}
473 was assessed every 30 min. Data were analyzed using the following modified 3-parameter
474 Gompertz equation: $y = A \exp\{- \exp[(\mu_m e/A)(\lambda - t)+1]\}$, where μ_m is the growth rate, λ the lag
475 time, and A the asymptote [10]. Data were fitted using a SigmaPlot® software (Systat Software
476 Inc., San Jose, CA). Time-kill experiments were carried out as described previously [9].
477

478 **Toxicity**
479 Cytotoxicity in HK2 cells which are an immortalized proximal tubule epithelial cell line from
480 normal adult human kidney (American Type Culture Collection (ATCC), Manass, VA), and in
481 human peripheral blood mononuclear cells was assessed using the CellTiter-Glo® luminescent
482 cell viability assay (Promega). For the peripheral blood mononuclear cells, blood from 3 separate
483 healthy donors was purchased from the Central Blood Bank (Pittsburgh, PA). The University of

Accepted Manuscript Posted Online

Antimicrobial Agents and Chemotherapy

AAC

484 Pittsburgh Institutional Review Board deemed that this study did not involve human subjects,
485 according federal regulations, and was therefore classified as exempt (IRB#: PRO1793975). To
486 assess cytotoxicity, cells were seeded at 5×10^3 to 5×10^4 cells/well in 96-well cell culture plates
487 containing ANY1 for 24 h before cell viability was measured.
488

489 **ACKNOWLEDGEMENTS**

490 This study was supported by a research grant from the National Institutes of Health grant number
491 R21AI123747. MLE was supported by T32DK061296 and TL1TR001858.

492
493
494
495
496
497
498
499
500
501
502
503
504
505
506
507
508
509

Downloaded from http://aac.asm.org/ on January 17, 2019 by guest

Antimicrobial Agents and Chemotherapy

Accepted Manuscript Posted Online

Antimicrobial Agents and Chemotherapy

AAC

Antimicrobial Agents and Chemotherapy

Downloaded from http://aac.asm.org/ on January 17, 2019 by guest

510 **REFERENCES**

511

512 1. The World Health Organization. Antibacterial agents in clinical development. (World Health
513 Organization, Geneva, Switzerland, 2017)
514 2. Kahan FM, Kahan JS, Cassidy PJ, Kropp H. 1974. The mechanism of action of fosfomycin
515 (phosphonomycin). Ann N Y Acad Sci. 235:364-386.
516 3. Sastry S, Doi Y. 2016. Fosfomycin: Resurgence of an old companion. J Infect Chemother.
517 22:273-280
518 4. Grabein B, Graninger W, Rodríguez Baño J, Dinh A, Liesenfeld DB. 2017. Intravenous
519 fosfomycin - back to the future. Systematic review and meta-analysis of the clinical
520 literature. Clin Microbiol Infect. 23:363-372.
521 5. Ito R, Mustapha MM, Tomich AD, Callaghan JD, McElheny CL, Mettus RT, Shanks RMQ,
522 Sluis-Cremer N, Doi Y. 2017. Widespread Fosfomycin Resistance in Gram-Negative
523 Bacteria Attributable to the Chromosomal *fosA* Gene. MBio 8:pii: e00749-17.
524 6. Bernat BA, Laughlin LT, Armstrong RN. 1997. Fosfomycin resistance protein (FosA) is a
525 manganese metalloglutathione transferase related to glyoxalase I and the extradiol
526 dioxygenases. Biochemistry. 36:3050-3055.
527 7. Rigsby RE, Rife CL, Fillgrove KL, Newcomer ME, Armstrong RN. 2004.
528 Phosphonoformate: a minimal transition state analogue inhibitor of the fosfomycin resistance
529 protein, FosA. Biochemistry. 43:13666-13673.
530 8. Ito R, Tomich AD, McElheny CL, Mettus R, Sluis-Cremer N, Doi Y. 2017. Inhibition of
531 fosfomycin resistance protein FosA by phosphonoformate (foscarnet) in multidrug-resistant
532 Gram-negative pathogens. Antimicrob Agents Chemother. 61: pii: e01424-17.

Accepted Manuscript Posted Online

533 9. Klontz EH, Tomich AD, Günther S, Lemkul JA, Deredge D, Silverstein Z, Shaw JF,
534 McElheny C, Doi Y, Wintrode PL, MacKerell AD Jr, Sluis-Cremer N, Sundberg EJ. 2017.
535 Structure and Dynamics of FosA-Mediated Fosfomycin Resistance in *Klebsiella pneumoniae*
536 and *Escherichia coli*. Antimicrob Agents Chemother. 61: pii e01572-17.

537 10. Alrowais H, McElheny CL, Spychala CN, Sastry S, Guo Q, Butt AA, Doi Y. 2015.
538 Fosfomycin Resistance in Escherichia coli, Pennsylvania, USA. Emerg Infect Dis. 21:2045-
539 2047.

540 11. Zwietering MH, Jongenburger I, Rombouts FM, van 't Riet K. 1990. Modeling of the
541 bacterial growth curve. Appl Environ Microbiol. 56:1875-1881.

542 12. The World Health Organization. Antimicrobial resistance: global report on surveillance
543 (World Health Organization, 2014).

544 13. Michalopoulos A, Virtzili S, Rafailidis P, Chalevelakis G, Damala M, Falagas ME. 2010.
545 Intravenous fosfomycin for the treatment of nosocomial infections caused by carbapenem-
546 resistant *Klebsiella pneumoniae* in critically ill patients: a prospective evaluation. Clin
547 Microbiol Infect. 16:184-186.

548 14. Tommasi R, Brown DG, Walkup GK, Manchester JI, Miller AA. ESKAPEing the labyrinth
549 of antibacterial discovery. 2015. Nat Rev Drug Discov. 14:529-542.

550 15. Richter MF, Drown BS, Riley AP, Garcia A, Shirai T, Svec RL, Hergenrother PJ. 2017.
551 Predictive compound accumulation rules yield a broad-spectrum antibiotic. Nature.
552 545:299-304.

553 16. Beharry Z, Palzkill T. 2005. Functional analysis of active site residues of the fosfomycin
554 resistance enzyme FosA from *Pseudomonas aeruginosa*. J Biol Chem. 280:17786-17791.

Downloaded from http://aac.asm.org/ on January 17, 2019 by guest

AAC

Antimicrobial Agents and Chemotherapy

Accepted Manuscript Posted Online

555 17. Kim DH, Lees WJ, Kempsell KE, Lane WS, Duncan K, Walsh CT. 1996. Characterization
556 of a Cys115 to Asp substitution in the Escherichia coli cell wall biosynthetic enzyme UDP-
557 GlcNAc enolpyruvyl transferase (MurA) that confers resistance to inactivation by the
558 antibiotic fosfomycin. Biochemistry. 35:4923-4928.
559 18. Zhu JY, Yang Y, Han H, Betzi S, Olesen SH, Marsilio F, Schönbrunn E. 2012. Functional
560 consequence of covalent reaction of phosphoenolpyruvate with UDP-N-acetylglucosamine 1-
561 carboxyvinyltransferase (MurA). J Biol Chem. 287:12657-12667.
562 19. Silver LL.2017. Fosfomycin: Mechanism and Resistance. Cold Spring Harb Perspect Med.
563 7: pii: a025262
564 20. Nilsson AI, Berg OG, Aspevall O, Kahlmeter G, Andersson DI. 2003. Biological costs and
565 mechanisms of fosfomycin resistance in *Escherichia coli*. Antimicrob Agents Chemother.
566 47:2850-2858.
567 21. Houde D, Berkowitz SA, Engen JR. 2011. The utility of hydrogen/deuterium exchange mass
568 spectrometry in biopharmaceutical comparability studies. J Pharm Sci. 100:2071-2086.

569
570
571
572
573
574
575
576

Downloaded from http://aac.asm.org/ on January 17, 2019 by guest

Antimicrobial Agents and Chemotherapy
AAC
Antimicrobial Agents and Chemotherapy

Accepted Manuscript Posted Online

Antimicrobial Agents and Chemotherapy

AAC

Antimicrobial Agents and Chemotherapy

Downloaded from http://aac.asm.org/ on January 17, 2019 by guest

577 **Table 1.** Data collection and refinement statistics. Overall values are reported with highest

578 resolution shell in parentheses.

Data Collection	$FosA^{KP}$ - ANY1	FosA3 - ANY1	$FosA^{KP}$ - ANY2
Resolution range	36.28 -3.178 (3.292 -3.178)	28.51 -3.502 (3.627 -3.502)	37.53 -1.85 (1.916 -1.85)
Space group	$C222_1$	$P4_32_12$	$P2_1$
Unit cell (a, b, c, α, β, γ)	120.399 197.615 117.027 90 90 90	73.181 73.181 123.818 90 90 90	44.765 68.837 90.312 90 90.464 90
Total reflections	98891 (9776)	61983 (5911)	154817 (15655)
Unique reflections	23338 (2128)	4588 (417)	45290 (4448)
Multiplicity	4.2 (4.3)	13.5 (13.7)	3.4 (3.5)
Completeness (%)	89 (98)	95 (100)	95 (97)
Mean I/sigma(I)	4.45 (1.23)	12.54 (1.66)	9.01 (1.76)
Wilson B-factor	47.47	125.71	17.25
R_{merge}	0.359 (1.25)	0.179 (1.95)	0.127 (0.829)
R_{meas}	0.408 (1.42)	0.186 (2.02)	0.151 (0.982)
CC1/2	0.953 (0.497)	0.998 (0.652)	0.995 (0.661)
CC*	0.988 (0.815)	0.999 (0.888)	0.999 (0.892)
Refinement			
Reflections used in refinement	21260 (2119)	4366 (417)	44418 (4437)
Reflections used for R-free	1105 (104)	222 (20)	2280 (223)
R_{work}	0.221 (0.294)	0.214 (0.389)	0.185 (0.277)
R_{free}	0.262 (0.318)	0.261 (0.439)	0.212 (0.294)
CC (work)	0.923 (0.766)	0.954 (0.652)	0.962 (0.786)
CC (free)	0.895 (0.814)	0.898 (0.445)	0.962 (0.772)
Number of non-hydrogen atoms	8654	2058	5073
Macromolecules	8406	1996	4273
Ligands	248	62	86
Protein residues	1094	271	551
Waters	0	0	163
RMS(bonds)	0.002	0.003	0.003
RMS(angles)	0.49	0.69	0.64
Average B-factor for macromolecules	41.88	123.29	20.11
Average B-factor for ligands	41.91	118.56	28.10

579

580

581

582

583

Accepted Manuscript Posted Online

Antimicrobial Agents and Chemotherapy

AAC

Antimicrobial Agents and Chemotherapy

584 **Table 2.** Dissociation constants (K_d) determined for ANY1 binding to wild-type and mutant

585 FosA3 measured by fluorescence quenching.

FosA3	Dissociation constant (K_d; nM)	Fold-change in K_d vs. wildtype (P value)
Wild type	440 ± 50	-
T9A	1580 ± 100	3.6 (< 0.05)
W34A	2620 ± 200	6.0 (<0.05)
S36A	1360 ± 130	3.1 (<0.05)
Y39F	870 ± 200	2.0
W46A	2480 ± 110	5.6 (< 0.05)
Y65F	780 ± 80	1.8
Y131A	4880 ± 770	11.1 <0.05)

586

587

588

589

590

591

592

593

594

595

596

597

598

599

600

601

602

Downloaded from http://aac.asm.org/ on January 17, 2019 by guest

Accepted Manuscript Posted Online

Antimicrobial Agents and Chemotherapy

AAC

Antimicrobial Agents and Chemotherapy

Downloaded from http://aac.asm.org/ on January 17, 2019 by guest

603 **Figure Legends**

604

605 **Fig. 1. Reaction schemes.** (**a**) Covalent modification of the MurA active site cysteine residue by
606 FOM; (**b**) FosA mediated nucleophilic addition of glutathione (GSH) to carbon-1 in the epoxide
607 ring of FOM; (**c**) Fluorescence quantification of GSH via conjugation with mBCl.

608

609 **Fig. 2. Thermodynamic and steady-state kinetic characterization of ANY1 binding to**
610 **FosA^{KP}**. (**a**) Chemical structure of ANY1, highlighting the pyrazolopyrimidine and pyrazole
611 moieties; (**b**) Representative run of ANY1 binding to FosA^{KP} as measured by ITC. The upper
612 panel represents the isotherms measured for 3860 s at 230 s injection intervals. The lower panel
613 shows a sigmoidal curve from an individual heat flow as a function of the total molar ratio
614 [(ANY1)/(FosA^{KP} monomer)] in the calorimeter cell. Binding isotherms were performed in
615 triplicate and corrected for heats of dilution; (**c**) Michaelis-Menten plot of FosA activity, in the
616 absence or presence of 5 μM, 10 μM or 20 μM ANY1, in which the GSH concentration was held
617 constant (25 mM) whereas the FOM concentration ranged from 0.5-25 mM. Data are shown as
618 the mean ± standard deviation from 3 separate biological replicates; (**d**) Michaelis-Menten plot
619 of FosA activity, in the absence or presence of 5 μM, 10 μM or 20 μM ANY1, in which the
620 FOM concentration was held constant (20 mM) whereas the FOM concentration ranged from 1-
621 25 mM. Data are shown as the mean ± standard deviation from 3 separate biological replicates.

622

623 **Fig. 3. Three-dimensional structures of FosA^{KP} or FosA3 in complex with ANY1 or ANY2.**
624 (**a**) Overlay of FosA^{KP} (green) and FosA3 (cyan), both in complex with ANY1. Two adjacent
625 FosA dimers are shown; (**b**) Residues in FosA^{KP} (green) and FosA3 (cyan) that interact with

Accepted Manuscript Posted Online

Antimicrobial Agents and Chemotherapy

AAC

Antimicrobial Agents and Chemotherapy

Downloaded from http://aac.asm.org/ on January 17, 2019 by guest

626 ANY1. Yellow dashed lines represent contacts shared between FosA and ANY1/FOM, while
627 black dashed lines represent contacts unique to FosA and ANY1. The pyrazolopyrimidine
628 moiety (pink) of the ANY1 molecule from the adjacent FosA molecule is also shown; (**c**)
629 Overlay of FosA^{KP} in complex with ANY1 (green) and in complex with FOM (light purple; pdb
630 entry 5V3D). Yellow dashed lines represent contacts shared between FosA and
631 ANY1/fosfomycin, while black dashed lines represent contacts unique to FosA and FOM; (**d**)
632 Structure of FosA^{KP} highlighting electron density surrounding two ANY1 molecules that link
633 adjacent FosA^{KP} active sites. Electron density was generated from composite omit maps,
634 contoured to 1.5 σ and carved to 2 Å from ANY1; (**e**) Overlay of FosA^{KP} in complex with ANY1
635 (green) or ANY2 (beige).
636
637 **Fig. 4. Hydrogen-deuterium exchange mass spectrometry of FosA^{KP} alone, or in complex**
638 **with FOM, ANY1 or ANY2**. (**a**) Differences in deuteration between peptides from FosA^{KP} and
639 FosA^{KP}-FOM; (**b**) Differences in deuteration between peptides from FosA^{KP} and FosA^{KP}-ANY1;
640 (**c**) Differences in deuteration between peptides from FosA^{KP}-ANY1 and FosA^{KP}-FOM; (**d**)
641 Differences in deuteration between peptides from FosA^{KP}-ANY1 and FosA^{KP}-ANY2. For (**a-d**),
642 peptides that contain residues from the GSH channel, dimer interface and K^+-binding loop are
643 highlighted. Differences in deuteration at individual time points are plotted as colored lines. The
644 98% confidence intervals for individual time points are plotted as dotted lines. The cartoon
645 representations on the right-hand side illustrate the FOM-, ANY1- or ANY2-induced changes in
646 hydrogen-deuterium exchange of FosA^{KP}. For each pair (Apo vs FOM, Apo vs ANY1, ANY1 vs
647 FOM, ANY1 vs ANY2), regions where the latter member of the pair demonstrates statistically
648 significant differences in relative deuteration are colored as follows: Regions with relative

Accepted Manuscript Posted Online

Antimicrobial Agents and Chemotherapy

AAC

Antimicrobial Agents and Chemotherapy

Downloaded from http://aac.asm.org/ on January 17, 2019 by guest

649 decreases in deuteration at the earliest time point (10 s) are colored dark blue; Regions with
650 relative decreases in deuteration only observed at later time points are colored light blue;
651 Regions with relative increases in deuteration at 10 s are colored dark red; Regions with relative
652 increases in deuteration at later time points are colored light red. The colors in the titles
653 correspond to the relative increase in protection mediated by that member.
654
655 **Fig. 5. Bacterial growth curves of *K. pneumoniae* I1, *P. aeruginosa* 75B2, *E. cloacae***
656 **YDC612, *S. marcescens* YDC760-2 or *E. coli* YD472 in the presence of a fixed**
657 **concentration of FOM and different concentrations of ANY1 (0-224 µg/mL).**
658 (**a**) Growth curve of *K. pneumoniae* I1 in the presence of 32, 64 or 128 µg/mL FOM and
659 different concentrations of ANY1 (0-224 µg/mL)**;** (**b**) Analysis of (**a**) illustrating changes in the
660 maximum growth asymptote (OD units) as a function of FOM (red-dotted lines), ANY1 (green
661 circles), ANY1+32 µg/mL FOM (yellow triangles), ANY1+64 µg/mL FOM (blue squares), and
662 ANY1+128 µg/mL FOM (pink diamonds); (**c**) Growth curve of *P. aeruginosa* 75B2, *E. cloacae*
663 YDC612, *S. marcescens* YDC760-2 or *E. coli* YD472 in the presence of 32, 64 or 128 µg/mL
664 FOM and different concentrations of ANY1 (0-224 µg/mL)
665
666 **Fig. 6. Bacterial growth curves of *K. pneumoniae* I1, *E. cloacae* YDC612, *S. marcescens***
667 **YDC760-2 or *E. coli* YD472 in the in the presence of a fixed concentration of ANY1 (112**
668 **µg/mL) and varying concentrations of FOM (0-1024 µg/mL).** (**a**) Maximum growth values
669 for *K. pneumoniae* I1 in the absence (black circles) or presence (white triangles) of 112 µg/mL
670 ANY1 and varying concentrations of FOM. The concentration of FOM that yielded 50 %
671 inhibition (i.e., IC_{50}) was determined by fitting data to hyperbolic ligand binding curve in Sigma

Accepted Manuscript Posted Online

Antimicrobial Agents and Chemotherapy

AAC

Antimicrobial Agents and Chemotherapy

Downloaded from http://aac.asm.org/ on January 17, 2019 by guest

672 Plot, and is reported in the figure legend; (**b**) Maximum growth values for *K. pneumoniae* I1 in
673 the absence (black circles) or presence (white triangles) of 112 µg/mL ANY1 and varying
674 concentrations of gentamicin (0-64 µg/mL); (**c**) Time-kill analysis of *K. pneumoniae* I1 in the
675 absence and/or presence of 112 µg/mL + 64 µg/mL; (**d**) Time-kill analysis of *K. pneumoniae* I1
676 in the absence and/or presence of 112 µg/mL + 64 µg/mL; (**e**) Time-kill analysis of *K.*
677 *pneumoniae* I1 in the absence and/or presence of 112 µg/mL + 64 µg/mL; (**f**) Maximum growth
678 values for *E. cloacae* YDC612 in the absence (black circles) or presence (white triangles) of 112
679 µg/mL ANY1 and varying concentrations of FOM (0-1024 µg/mL); (**g**) Maximum growth values
680 for *S. marcescens* YDC760-2 in the absence (black circles) or presence (white triangles) of 112
681 µg/mL ANY1 and varying concentrations of FOM (0-1024 µg/mL); (**h**) Maximum growth values
682 for *E. coli* YD472 in the absence (black circles) or presence (white triangles) of 112 µg/mL
683 ANY1 and varying concentrations of FOM (0-1024 µg/mL). All data presented in this figure are
684 shown as the mean ± standard deviation from at least 3 independent biological replicates.
685
686 **Fig. 7. ANY1 toxicity toward HK-2 cells and peripheral blood mononuclear cells (PBMC).**
687 (**a**) HK-2 cell viability following 24 h exposure to 1 mg/mL FOM or varying concentrations of
688 ANY1 (0-224 µg/mL). 10% DMSO was used as a positive control for toxicity. * denotes
689 statistically significant difference from media control ($p < 0.05$); (**b**) PBMC viability following
690 24 h exposure to 1 mg/mL FOM or varying concentrations of ANY1 (0-224 µg/mL); and 112
691 µg/mL ANY1 in combination with different concentrations of FOM. 10% DMSO was used as a
692 positive control for toxicity. * denotes statistically significant difference from media control ($p <$
693 0.05). All data presented in this figure are shown as the mean ± standard deviation from at least 3
694 independent biological replicates.

Accepted Manuscript Posted Online

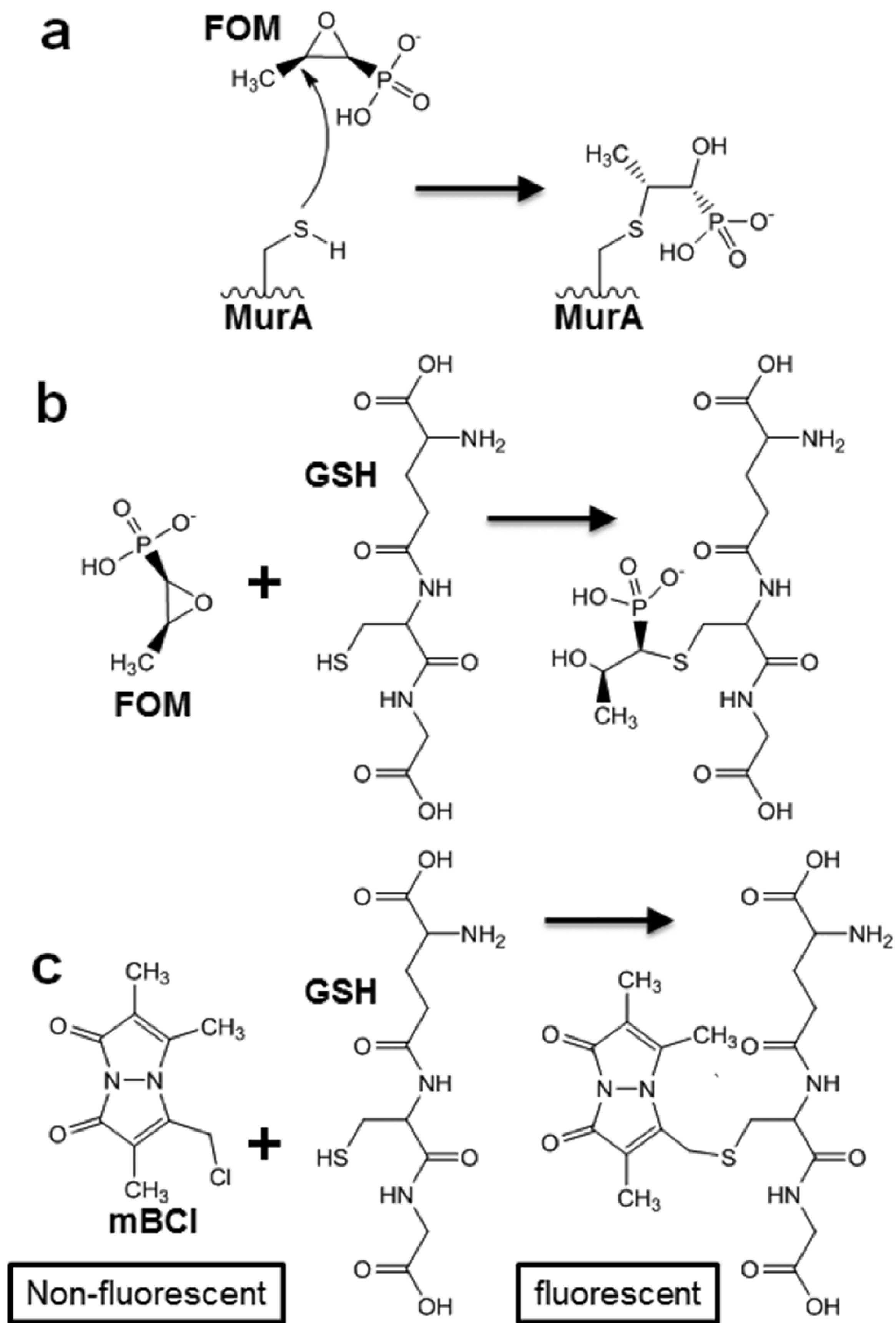

Downloaded from http://aac.asm.org/ on January 17, 2019 by guest

Accepted Manuscript Posted Online

Antimicrobial Agents and Chemotherapy

AAC

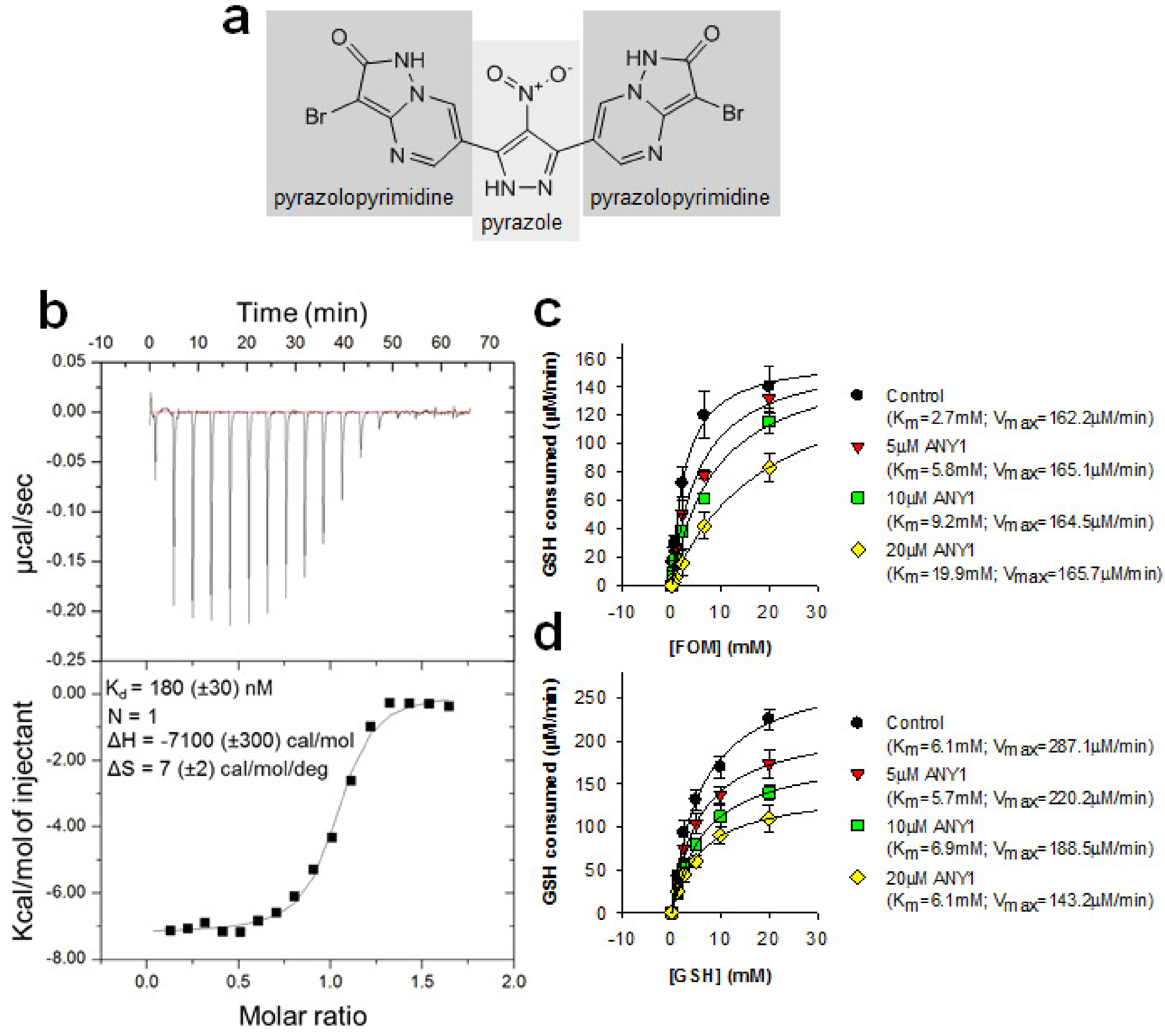

Downloaded from http://aac.asm.org/ on January 17, 2019 by guest

Antimicrobial Agents and Chemotherapy

Accepted Manuscript Posted Online

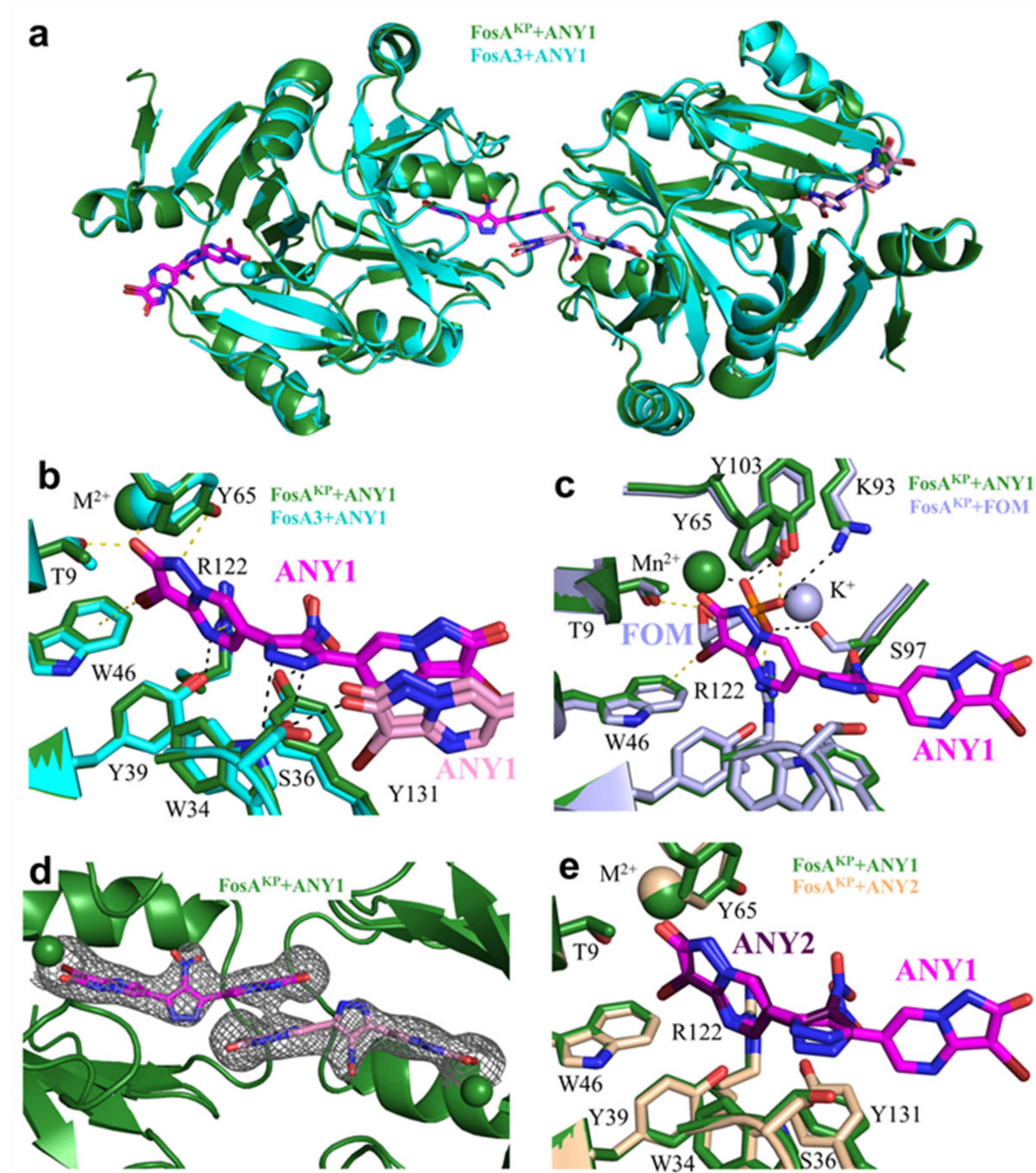

Downloaded from http://aac.asm.org/ on January 17, 2019 by guest

Antimicrobial Agents and Chemotherapy

AAC

Antimicrobial Agents and Chemotherapy

Accepted Manuscript Posted Online

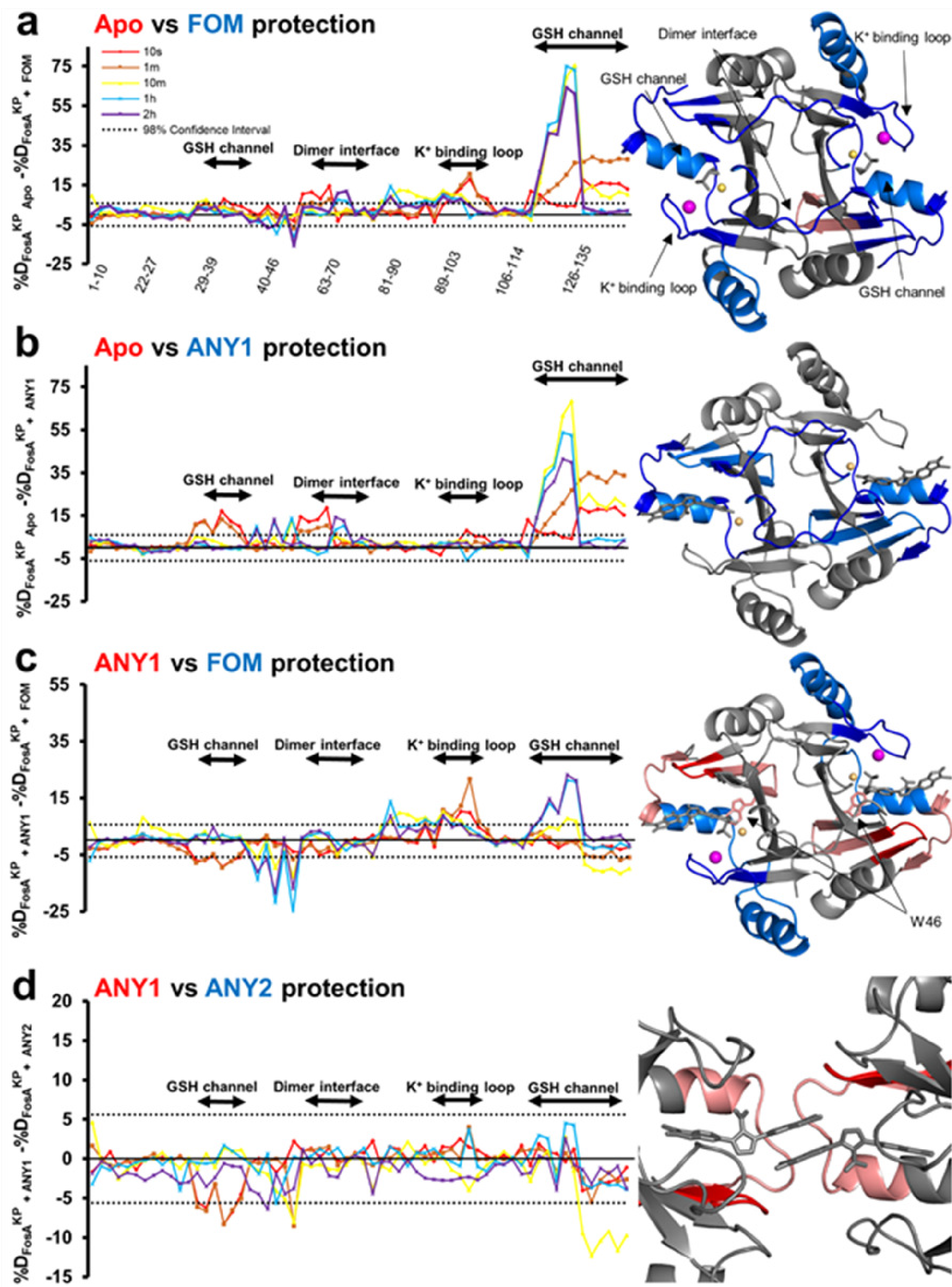

Downloaded from http://aac.asm.org/ on January 17, 2019 by guest

Accepted Manuscript Posted Online

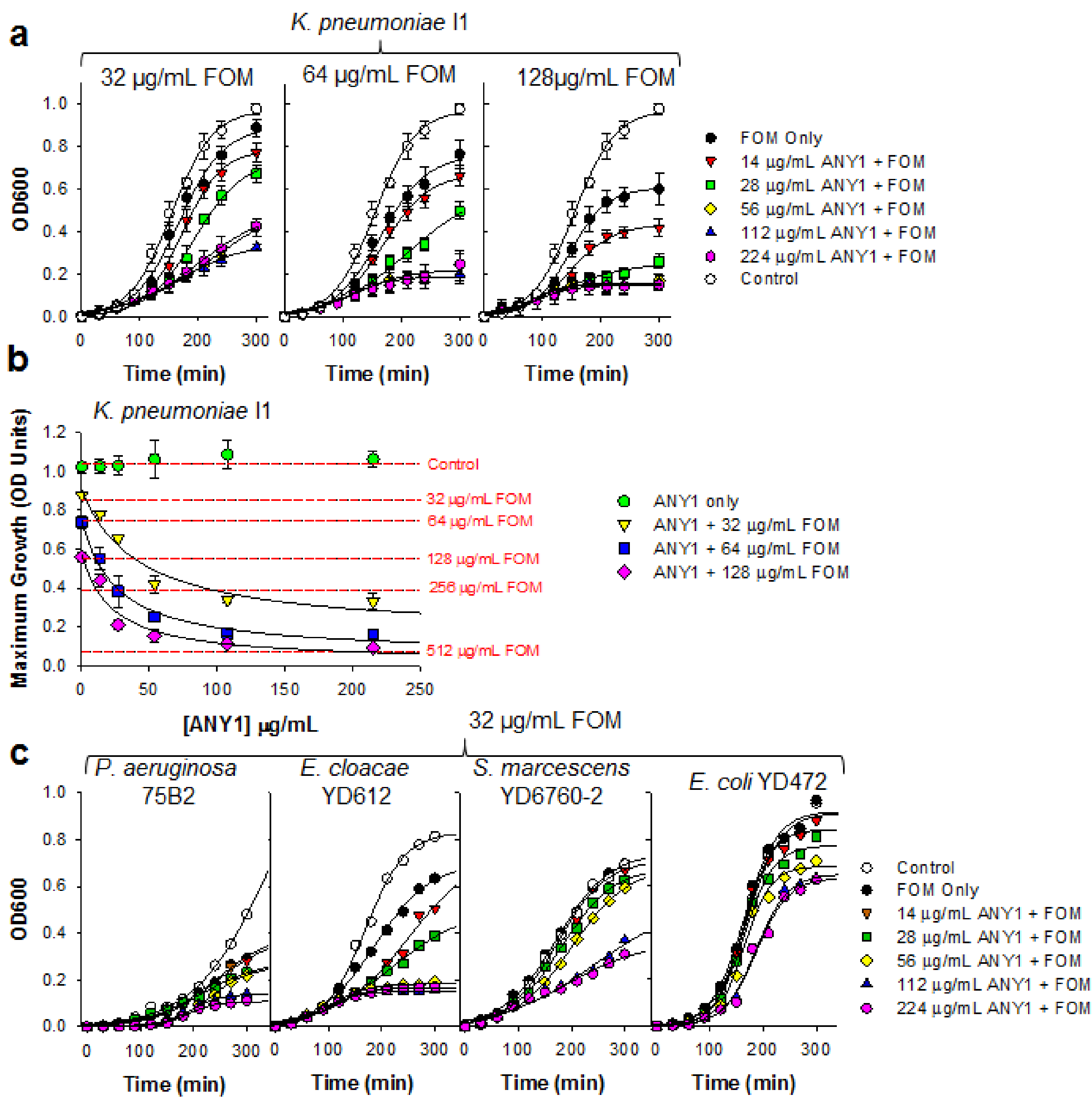

Downloaded from http://aac.asm.org/ on January 17, 2019 by guest

AAC
Antimicrobial Agents and Chemotherapy
Antimicrobial Agents and Chemotherapy

Accepted Manuscript Posted Online

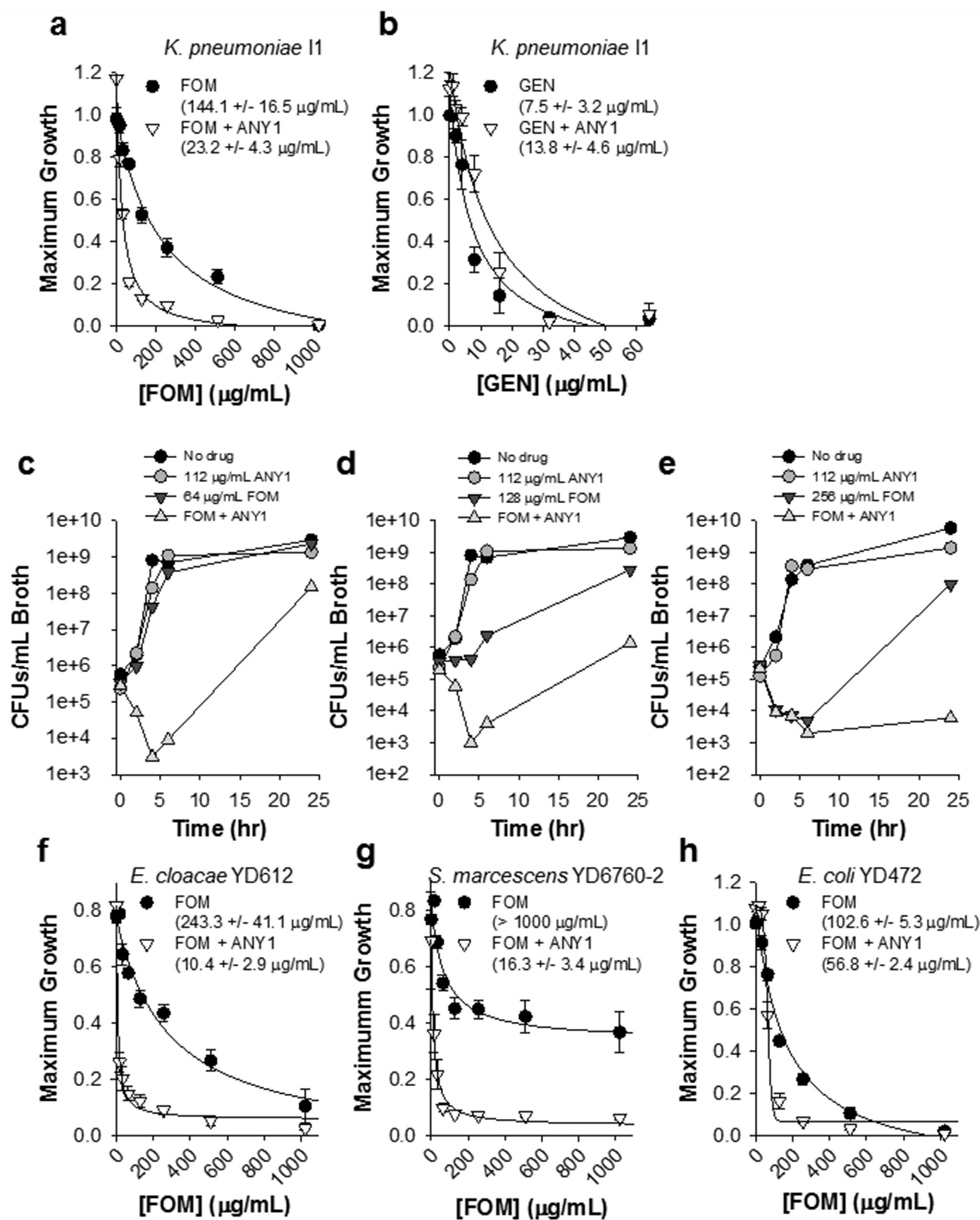

Antimicrobial Agents and Chemotherapy
AAC
Antimicrobial Agents and Chemotherapy
Downloaded from http://aac.asm.org/ on January 17, 2019 by guest

Accepted Manuscript Posted Online
Antimicrobial Agents and Chemotherapy
AAC
Antimicrobial Agents and Chemotherapy

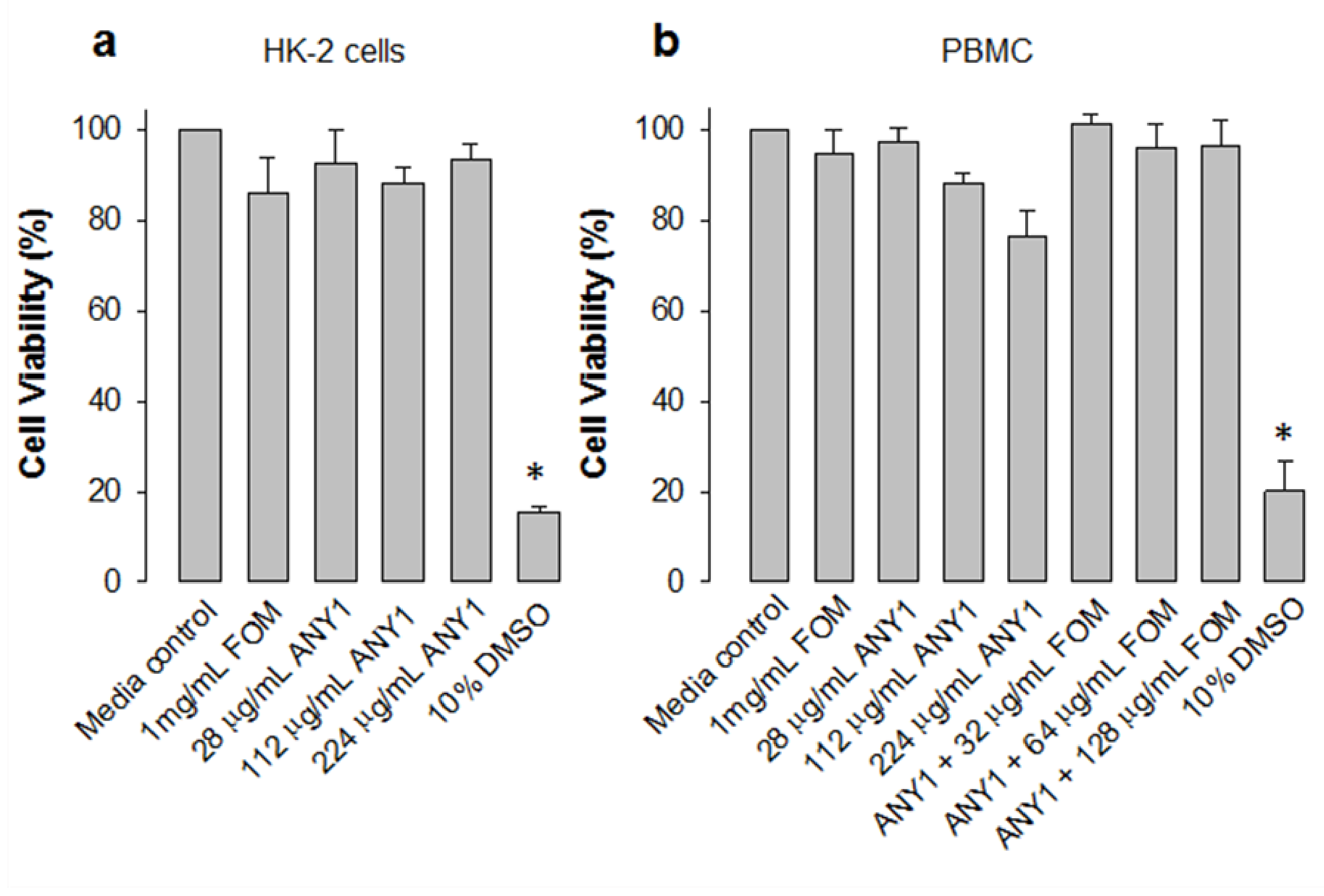

Downloaded from http://aac.asm.org/ on January 17, 2019 by guest